

# An Archetype for MRI guided Tele-interventions

Menelaos Karanikolas<sup>1,4</sup>, Eftychios Christoforou<sup>2,3</sup>, Erbil Akbudak<sup>2</sup>,  
Paul E. Eisenbeis<sup>2</sup>, and Nikolaos V. Tsekos<sup>2,\*</sup>

<sup>1</sup>Department of Anesthesiology, <sup>2</sup>Mallinckrodt Institute of Radiology,

<sup>3</sup>Department of Electrical and System Engineering Washington University,  
CB 8225, 4525 Scott Avenue, St. Louis, MO 63110, USA

<sup>4</sup>Department of Anaesthesiology and Critical Care Medicine, Faculty of  
Medicine University of Patras, Rion 26500, Greece

[tsekosn@mir.wustl.edu](mailto:tsekosn@mir.wustl.edu)

WWW home page: <http://www.cvil.wustl.edu/Staff/Tsekos/>

**Abstract.** The aim of this work is to evaluate a robotic system for remote performance of minimally invasive procedures with real-time magnetic resonance imaging (MRI) guidance inside clinical cylindrical scanners. In these studies, the operator had no physical access to the subject and used MR images and video from the observation camera in the scanner to control the robot. The control software allowed manual and semi-automated control modes and included components for collision avoidance, with the subject or the gantry of the scanner, and on-the-fly adjustment of the MR imagine plane to visualize the procedure. Studies were performed initially on phantoms and lastly on a pig inside a standard clinical cylindrical 1.5 Tesla MR scanner.

## 1 Introduction

### 1.1 MRI Guided Interventions

Magnetic Resonance Imaging (MRI) is one of several imaging modalities available for performing diagnostic and therapeutic image guided interventions (IGI). Compared to other competing modalities, MRI offers several advantages (1,2). (A) MRI offers a plethora of soft-tissue contrast mechanisms (e.g. perfusion, angiography and diffusion) which allow the assessment of both morphology and function. In addition MRI allows for monitoring the effects of procedures, such as thermal and cryo-ablations, which alter tissue properties. (B) MRI is the only true three-dimensional (3D) modality that allows oblique 3D or multislice imaging. (C) Compared to X-rays, it does not use ionizing radiation and therefore is safer for the patient and medical staff. When cylindrical MR scanners are used, a major limitation is the extreme magnetic environment and limited access to the patient. While open scanners offer direct access to the patient, these systems are limited by their

---

Please use the following format when citing this chapter:

Karanikolas, Menelaos, Christoforou, Eftychios, Akbudak, Erbil, Eisenbeis, Paul, Tsekos, Nikolaos, 2006, in IFIP International Federation for Information Processing, Volume 204, Artificial Intelligence Applications and Innovations, eds. Maglogiannis, I., Karpouzis, K., Bramer, M., (Boston: Springer), pp. 476–483

suboptimal image quality and low speed of image acquisition. To address the patient accessibility limitation of cylindrical scanners, remotely actuated and controlled robotic manipulators have been introduced. Several examples of such MR-compatible manipulators have been demonstrated, for brain biopsies (3), breast interventions (4-6), and general purpose (7,8).

### 1.2 Tele-Interventions based on MRI Guidance

As imaging modalities improve, and communication capabilities are becoming faster and more reliable, there may be potential for physicians to provide specialized diagnostic services, or even therapeutic procedures from a distance. As physician and equipment resources are distributed unevenly geographically, patients sometimes have to travel great distances to reach facilities with capability and expertise to provide specialized care. Traveling in order to receive care is not only a great inconvenience and expense for the patient, but may even contribute to deterioration of the disease. In addition, when time is of importance, the capability to provide treatment from a distance may allow for timely diagnosis and intervention.

Recently, the possibility of conducting interventions from a remote location is receiving attention (9,10). Performance of remote operations is a very complex and challenging task, from the technical and clinical point of view. Our work in this area focuses mainly on one aspect of this undertaking. Specifically, we are investigating whether a physician can perform an intervention based primarily on MR images without physical access to the subject. This paper describes an interventional system based on an MR-compatible manipulator and examines the feasibility of conducting spinal diagnostic and stereotactic procedures from a distance, i.e. with the physician in a location physically separate from the location of the patient. This is a pilot project, and should be looked at only as a feasibility study.

## 2 Overview of the Manipulator

Figure 1a reviews the overall layout of the interventional system, which is described in detail in (8). The system is composed of a seven degree-of-freedom (DOF) MR-compatible robot, hardware and software for its control. The manipulator has a Cartesian positioner, which resides in-front of the scanner (Fig. 1) and provides three orthogonal DOF (X, Y and Z), and an articulated arm with four DOF, which is deployed inside the gantry (Fig. 2). Two of these DOF are rotational ( $\theta_1$  and  $\theta_2$ ), resembling a dual "elbow" in-tandem, to set the Euler angle ( $\phi$ ) on the vertical plane. The third rotational DOF ( $\theta_3$ ) resembles a "wrist", orthogonal to the axis of  $\theta_2$  axis to set the other Euler angle ( $\theta$ ). These six DOF are actuated with ultrasonic motors. The seventh DOF is on the end-effector of the manipulator and sets the depth of insertion ( $\Delta$ ) with a manual cable-driven mechanism. The control software, reviewed in Fig. 4, was developed in the Simulink (The Mathworks Inc., Natick, MA) based xPC Target real-time environment and utilizes two dedicated personal computers (PC) (Fig. 1). The "Host PC" provides means for manual control, through a graphical user interface (GUI) or a master/slave device. It also generates and sends instructions to the "Target PC", for real-time control of the manipulator, and to the MR scanner, for adjustment of the position and orientation on of the imaging plane.

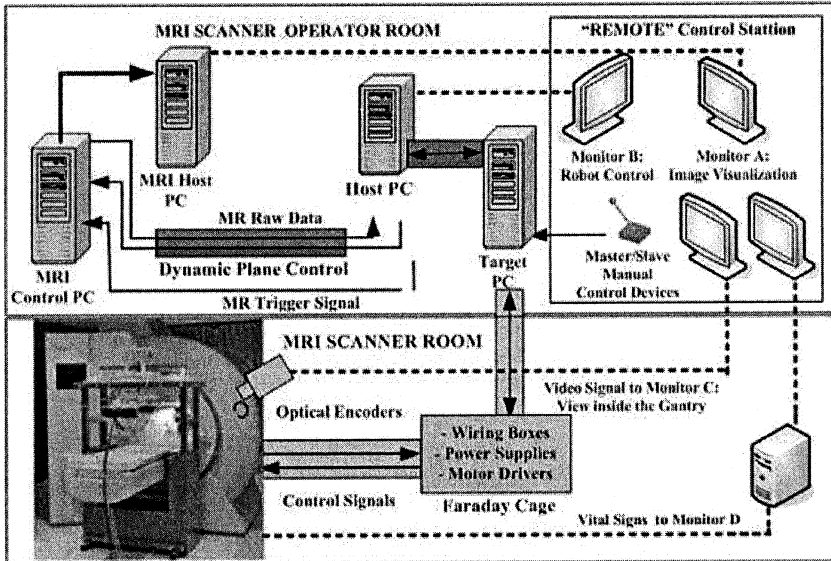


Fig. 1: The main components of the system and their connections.

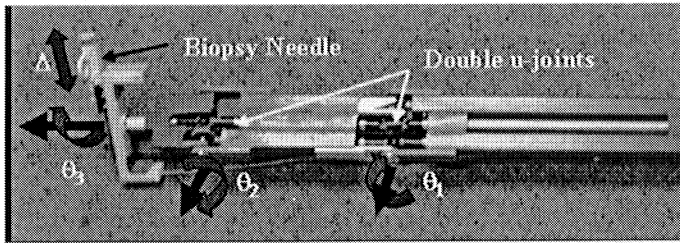


Fig. 2: Photograph of the distal end of the arm depicting its four DOF

Table 1: Characteristics of the Degrees of Freedom

DOF	Transmission	Operation	Backlash	Rigidity
X	Rack & Pinion	± 15 cm	~ 0 cm	~ 0 cm/Nm
Y	Lead Screw	± 9 cm	~ 0 cm	~ 0 cm/Nm
Z	Rack & Pinion	± 20 cm	~ 0 cm	~ 0 cm/Nm
$\theta_1$	Shaft and Bevel Gear	± 45 deg	± 2 deg	1.2 deg/Nm
$\theta_2$	Shaft, u-joints, Bevel Gear	± 45 deg	± 1.25 deg	2.6 deg/Nm
$\theta_3$	Shaft & u-joints	± 180 deg	± 3 deg	11.5 deg/Nm
$\Delta$	Cable	8 cm	~ 0 cm	~ 0 cm/Nm

### 3 Control Environment

Control of the manipulator is based on four elements which operate in synergy (Fig. 3). (a) A safety component which checks continuously to prevent collision of the manipulator with the gantry or the subject. (b) A procedure to register the position of

the manipulator relative to the coordinate system of the MR scanner. (c) A GUI human-machine interface for entering control commands. (d) Software which performs calculations for controlling the manipulator and updates the position and orientation of the imaging plane using the forward kinematics solutions.

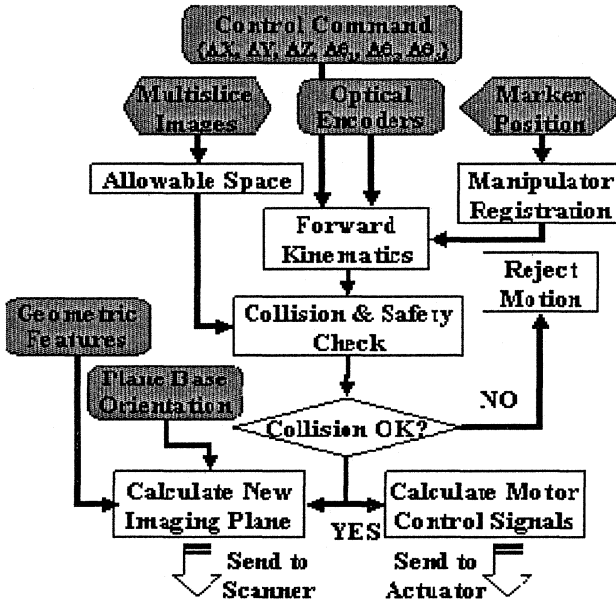


Fig. 3: Block diagram of the main processes of the control software. The input parameters are shaded in gray.

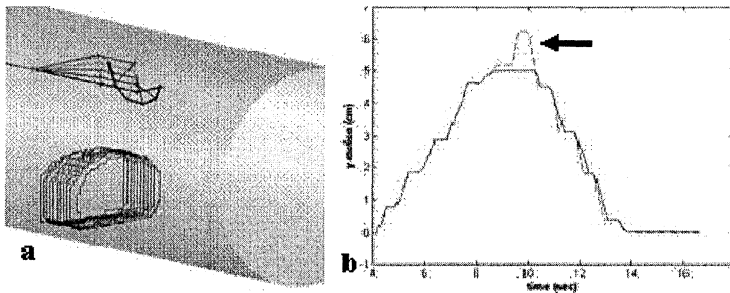


Fig 4: Example output of the safety control software showing the (a) exclusion zone and (b).example of a commanded (red dashed) and executed motion (black continuous line).

### 3.1 Safety Controls

The safety component uses a set of transverse slices to extract the boundaries of the subject, with an edge-detection (Canny-based) algorithm to generate the subject-defined maneuvering exclusion zone (Fig. 4a). The safety component reads the solution of the forward kinematics and continuously checks whether the current

position and any commanded motion are within the allowable maneuvering zone. Figure 4b shows example of the actuation of the Y (vertical) DOF. When the commanded motion causes the robot to enter in the exclusion zone, the safety routine prevents its execution and the robot remains idle (black arrow).

### **3.2 Human-Machine Interface**

Manual control of the manipulator was performed with a simple GUI with user-defined motion steps of 0.1 mm to 5 mm for the linear DOF and  $1^\circ$  to  $5^\circ$  for the rotational DOF. The motion instructions are then fed to the forward kinematics routine which calculates the position of the end-effector at the conclusion of the commanded motion. This solution is then sent to the safety component.

### **3.3 Manipulator-driven Control of the MR scanner**

For manipulator-driven control of the position and orientation of the imaging plane, the control software calculates the current position and orientation of the plane on which the interventional tool loaded on the end-effector will reside at the end of each step. Two types of manipulator-driven scanner control are available. With the computer-managed type, the Target PC continuously updates the imaging plane on-the-fly without any involvement by the operator. With the operator-managed type, the orientation of a slice remains unchanged during the actuation of a certain DOF to always image the end-effector during to actuation of this particular DOF.

## **4 Experimental Studies**

### **4.1 Set Up**

All experimental MR studies were performed on a 1.5 Tesla Sonata (Siemens Medical Solutions) using the body coil for RF pulse transmission and signal reception. To evaluate whether a physician can guide a procedure remotely without direct physical access to the subject, the interventionalist was located at the MR control room and had access to the following information and tools (fig. 1a). (a) MR images viewed on the MR scanner monitor and included windows shown pre-operation high-resolution and high-contrast images, and a window dedicated in viewing real-time updated low-contrast and high speed images. (b) Continuous video streaming on a dedicated monitor from a stationary camera located at the back side of the scanner (toward the head). (c) Continuous audio communication with one of the co-authors residing inside the MR scanner room. This individual was monitoring the system performance and, in particular, checking whether the needle appeared to bend or deviate for any other reason from its predefined path. This was deemed necessary since the black and white camera did not give a very clear depiction of the needle before it entered in the animal. (d) Robot control using a GUI on the monitor of the Host PC. In the operator room there is also a monitor which displays the main vital signs (EKG, blood pressure, respiratory rate and arterial oxygen saturation). Since the animal was euthanized in our experiments, we did not use this monitor.

#### 4.2 Phantom Studies

Registration of the manipulator to the scanner coordinate system was performed by measuring the coordinates of the center of a cross shaped MR-visible marker (made of 3% Gd-filled 3.1 mm diameter tubes), attached to a specific position on the end-effector). Computer-managed manipulator-driven dynamic imaging studies were performed on a phantom composed of a piece of beef with embedded two Gd-filled tubes (same as above) and a 500 cc saline bag rested on its side. Imaging was conducted with a true fast imaging with steady precession (TrueFISP) sequence (TR/TE/ $\alpha$  = 4.3 ms/2.15 ms/30°; slice = 8 mm; matrix = 128x256; FOV = 260x260mm<sup>2</sup>; pixel size = 1.5x1.5 mm<sup>2</sup>). Two 3.1 mm diameter Gd-filled tubes were attached to the end-effector for viewing the otherwise MR-invisible manipulator.

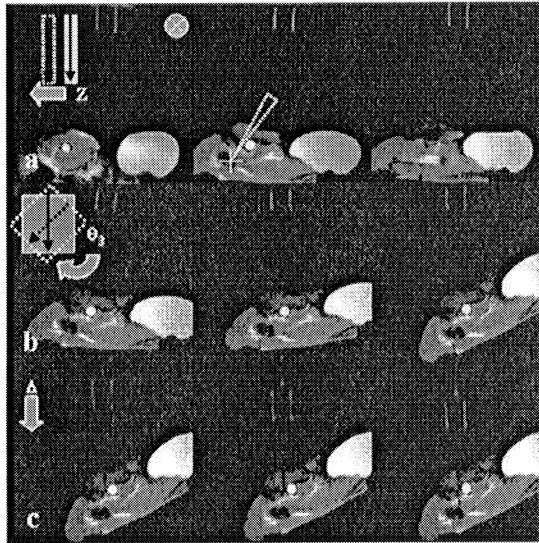


**Fig. 5:** Selected frames from an image-guided procedure monitored with the computer-managed manipulator-driven dynamically controlled TrueFISP.

Figure 5 shows a study with the computer-managed manipulator-driven dynamic update of the imaging plane. Initially, panel 4a, the operator moved the manipulator over the phantom, to select a target (cross) and a direction of insertion, approximately within the dashed-line triangle. Maneuvers were then performed as example rotating the wrist joint (3b) to align the needle with the planned strategy of target acquisition. All the specified targets were reached with an accuracy of 3.2 mm, relative to the center of structures ranging in size from between 1 cm and 1.4 cm diameter. The in-plane orientation accuracy of the path was within 2.5° for each one of the two Euler angles.

#### 4.3 Spinal procedure

The system was tested for the performance of a spinal procedure on a euthanized pig. Scout images were obtained with a spin-echo (SE) sequence (TR/TE = 500ms/15ms;

slice thickness = 4 mm, acquisition matrix 384 x 512 and a pixel size  $1.3 \times 1.3 \text{ mm}^2$ ) for preliminary localization of the target tissue, which, in this particular experiment was the spinal canal in the lumbar area. Once the area of intervention was defined, the arm of the robot was advanced into the cylindrical MRI scanner.

The desired trajectory of the MRI-compatible 20 G needle followed a slightly paramedian approach, so that the needle could avoid the spinous processes of the lumbar vertebral bodies, and could advance towards the spinal canal without encountering any bony structures in its projected path. The selected trajectory was defined by two points: (a) the entry point, which was marked by the interventional physician on the transverse MR image at skin depth, and (b) the destination point, located in the outer portion of the spinal canal in the area of the posterior epidural space. After the trajectory was defined on the images, the physician maneuvered the remote manipulator until the long axis of the needle was aligned with the indicated trajectory as confirmed by MR imaging, the needle was gradually advanced, under intermittent MRI imaging,. Once the needle advanced approximately 2 mm short off the total length of advancement, MR images were collected to confirm proximity of the tip of the needle to the target tissue. Based on these images, the needle was further advanced to reach the targeted spinal canal (Fig. 5). The entire procedure, including initial scouting images, definition of the needle trajectory, manipulator alignment and, finally, needle advancement until it reached the target took approximately 45 minutes.

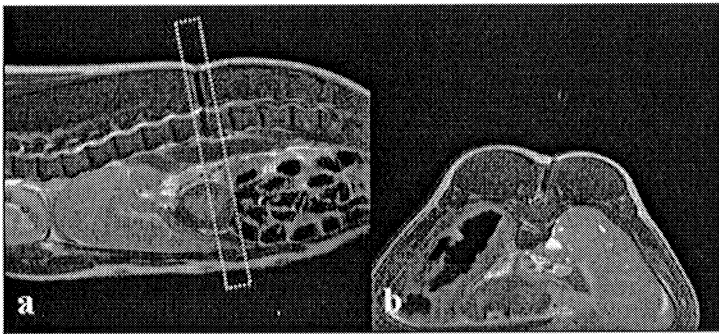


**Fig. 6:** Selected slices showing (a) an oblique sagittal view of the pig's abdomen and (b) an oblique transverse. The white box in (a) indicates the position of the slice shown in (b). Note the MR compatible needle as it enters and reaches the spinal canal.

## 5 Discussion and Conclusions

A prototype system is presented for performing minimally invasive interventions with real-time MR guidance inside a cylindrical MR scanner using a seven DOF robotic manipulator. Experiments were performed to assess whether an interventionalist can perform a procedure just by using MR images and position information from the robot control software but without physical access to the subject. At this early stage, the project is focused on the procedural aspect and the

work-load of combining robotics with MR imaging to perform a procedure without physical presence in the operating suite. Therefore, certain technical aspects critical for a clinical implementation of the system, such as the technology used for remote connection, were not addressed (9,10).

This pilot project pointed to certain improvements of this system including additional cameras \for better visualization of the area inside the gantry of the scanner and improved voice communication since; the latter is important since the MR room is extremely noisy during data acquisition. The system should also have a mechanism to compensate for patient movement, regardless of whether this movement is smooth and predictable (e.g. respiratory movement) or unpredictable to ensure accuracy of needle tip position and patient safety.

**Acknowledgments:** This work was supported in part (MR pulse sequences and real-time reconstruction hardware/software) by the NIH grant RO1HL067924. NVT also thanks the Special Secretary General of the Secretariat of Operational Programs, Ministry of Health, Greece.

## References

1. Debatin-G.Adam JF, editor. *Interventional Magnetic Resonance Imaging*: Springer; 1998.
2. Jolesz F, Kahn T, Lufkin R. Genesis of interventional MRI. *J Magn Reson Imaging* 1998;8(1):2.
3. Masamune K, Kobayashi E, Masutani Y, Suzuki M, Dohi T, Iseki H, Takakura K. Development of an MRI-compatible needle insertion manipulator for stereotactic neurosurgery. *J Image Guid Surg* 1995;1(4):242-248.
4. Kaiser WA, Fischer H, Vagner J, Selig M. Robotic system for biopsy and therapy of breast lesions in a high-field whole-body magnetic resonance tomography unit. *Invest Radiol* 2000;35(8):513-519.
5. Felden A, Vagner J, Hinz A, Fischer H, Pfleiderer SO, Reichenbach JR, Kaiser WA. ROBITOM-robot for biopsy and therapy of the mamma. *Biomed Tech (Berl)* 2002;47(Suppl 1 Pt 1):2-5.
6. Larson BT, Erdman AG, Tsekos NV, Yacoub E, Tsekos PV, Koutlas IG. Design of an MRI-compatible robotic stereotactic device for minimally invasive interventions in the breast. *J Biomech Eng* 2004;126(4):458-465.
7. Hempel E, Fischer H, Gumb L, Hohn T, Krause H, Voges U, Breitwieser H, Gutmann B, Durke J, Bock M, Melzer A. An MRI-compatible surgical robot for precise radiological interventions. *Comput Aided Surg* 2003;8(4):180-191.
8. Tsekos NV, Ozcan A, Christoforou E. A Prototype Manipulator for MR-guided Interventions Inside Standard Cylindrical MRI Scanners. *J Biomech Eng* 2005;127:972-980.
9. Seibel RM, Melzer A, Schmidt A, Plabetamann J. *Computed Tomography- and Magnetic Resonance Imaging: Guided Microtherapy*. *Semin Laparosc Surg* 1997;4(2):61-73.
10. Marescaux J, Leroy J, Gagner M, Rubino F, Mutter D, Vix M, Butner SE, Smith MK. Transatlantic robot-assisted telesurgery. *Nature* 2001;413(6854):379-380.